## NOTATION

$\theta$, equilibrium contact angle; $\sigma$, surfacetension of liquid; $K(r)$, local value of the surface curvature; $P_0$, capillary pressure of the drop at equilibrium; R, radius of curvature; $h(r)$, variable film thickness; $\Pi(h)$, disjoining pressure; $t_1$, radius for the action of surface forces; $h_0$, thickness of the equilibrium film on the surface; a and $t_0$, parameters which determine the change of the disjoining pressure.

## LITERATURE CITED


1. B. D. Summ and Yu. V. Goryunov, Physical–Chemical Bases of Wetting and Flow [in Russian], Moscow (1976).
2. W. Bascom, R. Cottington, and C. Singleterry, Contact Angle Wettability and Adhesion, E. W. Fowkes (ed.), American Chemical Society (Advances in Chemistry Series No. 43), Washington, DC (1964).
3. P. G. DeGennes, "Wetting: statics and dynamics," Rev. Mod. Phys., 57, 827-863 (1985).
4. V. I. Pshenitsyn, M. I. Abaev, and N. Yu. Lyzlov, Ellipsometry in Physical–Chemical Investigations [in Russian], Leningrad (L986).
5. V. P. Zolotarev, V. N. Morozov, and E. V. Smirnova, Handbook of Optical Constants of Natural and Industrial Materials [in Russian], Leningrad (1984).
6. J. R. Vig, Ultraviolet/Ozone Cleaning of Surfaces, Surface Contamination Genesis, Detection, and Control, K. L. Hittal (ed.), Vol. 1 (1979), pp. 235-255.
7. D. N. Vandyshev and S. G. Skakun, Thesis Report at the All-Union Academic Seminar "Spectroscopic Methods of Surface Analysis" [in Russian], Chelyabinsk (1990), pp. 32-33.
8. G. L. Chelidze, A. I. Derevyanko, and A. D. Kurilenko, Electric Spectroscopy of Heterogeneous Systems [in Russian], Kiev (1977), p. 232.
9. B. V. Deryagin, N. V. Churaev, and V. M. Muller, Surface Forces [in Russian], Moscow (1985).
10. V. M. Starov and N. V. Churaev, Kolloid. Zh., 42, 703-710 (1980).


# NONSTEADY FLOW OF A VAPOR–DROP FLOW IN A HEATED CHANNEL


V. E. Kroshilin and Ya. D. Khodzhaev



UDC 532.529.5



Flow of a vapor–drop mixture in a heated channel is studied under steady and nonsteady conditions using a model which considers direct thermal interaction of drops with the heating surface.


In various heated channels using a two-phase working fluid as well as in accidental situations a vapor–droplet flow can develop, as has been mathematically modeled in a large number of studies – an overview can be found in [1]. A complete model for description of a vapor–drop flow in a heated channel under steady-state conditions was presented in [1]. That model considered direct thermal interaction of drops with the heating surface, and the temperature of the superheated vapor was found from the energy equation, including the thermal flux from the heating surface into the vapor and the thermal flux from the vapor to the drops. In the present study, using a model analogous to that of [1], we will consider the flow of a vapor–drop mixture under steady and nonsteady conditions. The system of equations for the flow of vapor–drop mixture [1] (assuming that the flow is not in thermodynamic equilibrium, the vapor velocity is equal to the drop velocity, and breakup and combination of drops are absent) has the form:

$$\begin{gathered}\partial(\rho_i^0\alpha_i)/\partial t+\partial(\rho_i^0\alpha_i v)/\partial z=J_{ij},\\ \partial(u_i\rho_i^0\alpha_i)/\partial t+\partial(u_i\rho_i^0\alpha_i v)/\partial z=-J_{ij}u_{is}+\alpha_i p/\rho_i^0\, d\rho_i^0/dt-Q_{i\sigma}+Q_{w1},\\ \partial n/\partial t+\partial(nv)/\partial z=0,\end{gathered}\tag{1}$$


Mechanics Institute, M. V. Lomonosov State University, Moscow.


Translated from Inzhenerno-Fizicheskii Zhurnal, Vol. 61, No. 6, pp. 939-946, December, 1991. Original article submitted August 23, 1990.

$$\rho(\partial v/\partial t + v\partial v/\partial z) = -F_w - \rho g - \partial p/\partial z,$$

$$Q_{1\sigma} + Q_{2\sigma} = J_{21}l,$$

where the subscript i denotes the phase described by the given quantity: i = 1, vapor; i = 2, drops.

The characteristic time for establishment of stationary velocity and pressure profiles is much less than the time for establishment of steady volume concentration profiles [1], which are equal to the characteristic times of processes important in practice. Consideration of this fact allows [1] reduction of the original system of differential equations to quasisteady form, i.e., allows neglect of the derivatives $\partial p/\partial t$ and $\partial v/\partial t$. Analysis of results of the experimental studies of [1] shows that the characteristic time for establishment of steady values of the friction force between flow and wall, equal to the "growth" time of the nonsteady boundary layer in the channel ($t_f \sim 0.001$-$0.01$ sec), is much less than the characteristic time of the processes important in practice. Therefore, to determine the friction force a relationship obtained in experiments under steady state conditions was used.

To determine heat exchange between the vapor and drops $Q_{1\sigma}$ we find (approximately) the slippage of the drops relative to the vapor $v_{12}$. This slippage can be found, following [1], from the condition that the acceleration of drops due to the vapor–drop friction force be equal to the acceleration of the mixture. To do this we make use of the equation of drop momentum

$$(\pi d_d^3/6)\rho_2^0\, dv/\partial t = c_f \pi d_d^2 \rho_1^0 v_{12}^2/8. \tag{2}$$

The resistance coefficient can be calculated with the expression [1]:

$$\text{for} \quad \mathrm{Re}_{12} \leqslant 1 \quad C_f = 16/\mathrm{Re}_{12},$$

$$\text{for} \quad \mathrm{Re}_{12} > 1 \quad C_f = 48(1 - 2{,}2/\sqrt{\mathrm{Re}_{12}})/\mathrm{Re}_{12},$$

$$\mathrm{Re}_{12} = \rho_1^0 v_{12} d_d/\mu_1.$$

Equation (2) is solved numerically at each step together with system (1).

The heat flux from the vapor to the drop surface is calculated using the following expressions [1]:

$$Q_{1\sigma} = 6\alpha_2\lambda_1 \mathrm{Nu}_{1\sigma}(T_1 - T_2)/d_d^2, \quad T_2 = T_s(p),$$

$$\mathrm{Nu}_{1\sigma} = 2 + 0{,}6\,(\mathrm{Re}_{12})^{0,5}\,\mathrm{Pr}_1^{0,4}, \quad \mathrm{Pr}_1 = \mu_1 C_1/\lambda_1.$$

Calculations show that as a rule the amount of slippage does not exceed 5% of the flow velocity and can be neglected in the motion equation. However this slight slippage markedly increases the number $\mathrm{Nu}_{1\sigma}$.

The friction force between the vapor–drop flow and the wall can be represented in the form [2]:

$$F_w = C_{1f}\rho_1^0 v^2/(2d),$$

$$\text{for} \quad \mathrm{Re}_1 \leqslant 10^5 \quad C_{1f} = 0{,}3164/\mathrm{Re}_1^{0,25},$$

$$\text{for} \quad \mathrm{Re}_1 > 10^5 \quad C_{1f} = 0{,}0032 + 0{,}221/\mathrm{Re}_1^{0,237}.$$

It should be noted that in the one-dimensional formulation of the problem considered herein flow interaction with the wall (force and thermal) is considered by empirical expressions (describing molecular and turbulent transport).

Heat removal from the heated surface per unit volume of mixture $Q_w$ is composed of heat removal by the vapor $Q_{w1}$ and direct removal by drops $Q_{w2}$:

$$Q_w = Q_{w1} + Q_{w2}. \tag{3}$$

The heat influx per unit volume of vapor–drop mixture due to thermal flux between the wall and vapor can be calculated with the expression presented in [2]:

$$Q_{w1} = 4\lambda_1 \mathrm{Nu}_{w1}(T_w - T_1)/d^2,$$

$$\mathrm{Nu}_{w1} = 7{,}6 - 3{,}6/\lg(\mathrm{Re}_1) + 0{,}0096\,\mathrm{Re}_1^{0{,}87}\,\mathrm{Pr}_1^n,$$

where $n = 0.4 + 0.5/(2\mathrm{Pr}_2 + 1)$.

In calculating heat removal by drops from the wall, following [3], the following mechanism was assumed: the drops approach the wall within a distance $\delta_*$ (vapor layer thickness) over a time $t_d$ (equal to the period of free drop oscillations) and move away from the wall, carrying off heat transmitted through the vapor gap:

$$Q_{w2} = \pi d_d^2 \lambda_1 t_d N_w (T_w - T_2)/(4\delta_*).$$

The period of free drop oscillations $t_d$ is given by the expression [3]:

$$t_d = \pi \sqrt{\rho_2^0 d_d^3/\sigma}\,/4.$$

The number of drops approaching the wall per unit time per unit channel volume $N_w$ was calculated using an experimental dependence for drop precipitation intensity [1]:

$$N_w = J_{2w}6/(\pi d_d^3 \rho_2^0),\quad J_{2w} = 4\rho_2^0 \alpha_2 v J_{32}^*/d,$$

$$J_{32}^* = 8\cdot 10^{-3}\alpha_2^{-0,1}\,\mathrm{Re}_1^{-0,12}\,f(\Pi),$$

$$f(\Pi) = \Pi^{1/2} \text{ for } \Pi \leqslant 1,\ f(\Pi) = \Pi \text{ for } \Pi > 1,$$

$$\Pi = 0{,}16\,\sigma(\rho_1^0/\rho_2^0)^{0,26}/(v\sqrt{\mu_1\mu_2}).$$

Generally speaking, the thickness of the interlayer between the drops and wall $\delta_*$ should change along tube length, since the wall $T_w$ and vapor $T_1$ temperatures change intensely over tube length and this affects the flow parameters. However, calculations with a constant interlayer thickness $\delta_* = 0.7$ μm agree well with the experimental data of [4], which were obtained over a quite wide range of regime parameters. Consequently for the given conditions the thickness of the vapor interlayer $\delta_*$ is constant for all segments of the tube where the vapor–drop flow moves at all times. It should be noted that the vapor interlayer thickness $\delta_*$ is the only parameter which was chosen by matching theoretical and experimental data.

The drop diameter was determined from the following expression obtained from the first and third equations of system (1):

$$dd_d/dt = -J_{21}d_d/(3\rho_2^0\alpha_2).$$

The initial drop diameter was determined from the condition of equality of the drop Weber number to the critical Weber number, $\mathrm{We}_* = 15$ [1].

The thermophysical properties of the vapor were determined by approximating the tabular data of [5].

Under steady-state conditions the temperature of the heated surface was found from the condition of equality of the heat liberation in the tube walls to the heat flux into the mixture.

With consideration of the assumptions made above regarding the quasi steady state, system (1) reduces to several transport equations and algebraic relationships. As boundary conditions at the beginning of the vapor–drop flow (first calculation cell) all flow parameters were specified (for the transport equations these conditions are sufficient). As initial conditions for system (1) one usually uses a flow parameter distribution corresponding to steady conditions (obtained by solution of Eq. (1) without consideration of time derivatives). To solve the transport equations $(\partial\rho/\partial t + \partial(\rho v)/\partial z = J)$ the simplest possible explicit finite difference schemes were used: $\partial\rho/\partial t$ was replaced by $(\rho_m^n - \rho_m^{n-1})/\Delta t$; $\partial(\rho v)/\partial z$ was replaced by $((\rho v)_m^{n-1} - (\rho v)_{m-1}^{n-1})/\Delta z$, where the subscript m indicates the number of the calculation cell and the superscript n indicates the number of the time layer, $\Delta t$ is the step in time and $\Delta Z$, the step in coordinate.

The calculation accuracy was determined by verifying preservation of balance relationships and performing calculations with finer scale calculation grids. The calculations

showed that upon division of the calculation region into 500 cells the error does not exceed several percent.

To verify the vapor–drop flow model the calculation results were compared to experimental data from [4]. In those experiments the vapor–gas flow occurred in various regimes, the main ones of which were flow of underheated liquid, bubble flow, dispersed-ring, and vapor–drop flows. The proposed model was used to describe the vapor–drop flow, while the model presented in [6] was used for the other three regimes. The flow parameters at the beginning of the vapor–drop flow regime were calculated using the laws of conservation of vapor and liquid expenditure using the parameters at the end of the dispersed-ring flow (boundary conditions). In the experiments the ascending steady-state vapor–drop flow moved in a vertical tube with inner diameter d = 0.0126 m, length L = 6 m, wall thickness $\delta$ = 1 mm at an input pressure p = 6.9 MPa. The mass flow rate was varied over a wide range $\rho^W$ = 350-5500 kg/(m$^2$·sec), total thermal flux was varied (Q = 81-410 kW), and water subheat $\Delta T$ at input was varied from 10 to 40°C. The experiments measured the temperature distribution over the length of the tube wall. It should be noted that the experimental data encompass a wide range of regime parameters, significantly exceeding the parameter range of the energy equipment. The calculated and experimental wall temperature values agreed satisfactorily (within 15-20%). Therefore, the range of applicabiility of the problem formulation presented is quite wide. The calculation results show that the change in wall temperature in the postcrisis region is controlled by two basic mechanisms. The first mechanism functions as follows. Because of increase in flow velocity along the length of the tube the heat liberation coefficient between the heated surface and the vapor increases and the difference between the temperatures of the heated surface and vapor decreases (since the thermal flux is constant over length). Because of this mechanism the temperature of the heated surface should fall, since the vapor temperature does not increase intensely along channel length. The second mechanism consists of the following. At the beginning of the vapor–drop flow, as the calculations show, the drops make a significant contribution to heat liberation. The droplet mass flow rate decreases over channel length and heat removal from the heated surface by drops decreases. The sum of heat removal by drops and vapor is constant along channel length (and equal to the heat liberated into the tube walls). Therefore, heat removal by vapor must increase over length. In light of this mechanism the temperature of the heated surface should increase.

Figure 1 shows a characteristic distribution of vapor–drop flow parameters. It is evident that heat removal by drops $Q_{w2}$ decreases along tube length while heat removal by the vapor $Q_{w1}$ increases. This leads to an increase in temperature of the heated surface, i.e., in the given conditions the main effect on temperature change is exerted by the second mechanism described above.

The calculation results show that for a vapor–drop flow (in the range of regime parameters corresponding to practical problems) the Nusselt number Nu for heat exchange between the vapor and drops is significantly (up to five times) larger than the Nusselt number obtained without consideration of the relative motion of the drops (Nu = 2). This refers to a small relative velocity, comprising less than 5% of the flow velocity.

It should be noted that with increase in the total flow rate of vapor–liquid mixture the initial drop diameter decreases and the relative drop velocity also decreases. Therefore, the effect of relative motion on heat exchange between drops and vapor decreases.

As a rule the vapor–drop flow regime corresponding to postcrisis heat exchange develops from preceding flow regimes corresponding to heat exchange where heat removal from the heated surface is significantly better. Motion of the heat liberation crisis front (the section where the precrisis heat exchange is replaced by post-crisis) is determined to a significant degree by transport of heat along the tube wall from the post-crisis region where heat removal is difficult, to the pre-crisis region where heat removal is significantly better. Estimates indicate that the width of the region where heat transport along the tube walls is significant is very small, $\Delta \ll 0.1$ mm (this is also confirmed by results of calculations performed below). In this narrow region the temperature change is of the order of 300-500°C. Consequently, the temperature gradient along channel length is very high and significantly greater than the temperature gradient along tube radius. Therefore, to describe heat transport in this region we will use an approximate one-dimensional thermal conductivity equation for the mean over the radius of the tube wall temperature (for the conditions considered here the change in tube wall temperature along radius does not exceed 50°C):

$$c_w \rho_w \partial T_w / \partial t = \lambda_w \partial^2 T_w / \partial z^2 + q - Q_w d/(4\delta). \quad (4)$$

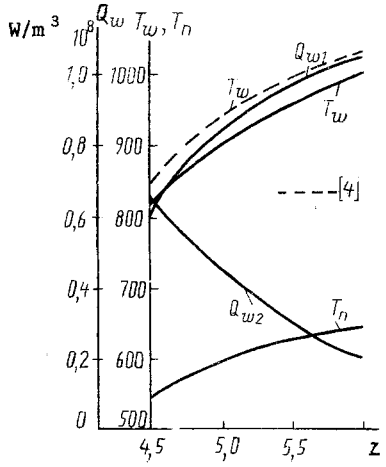


Fig. 1

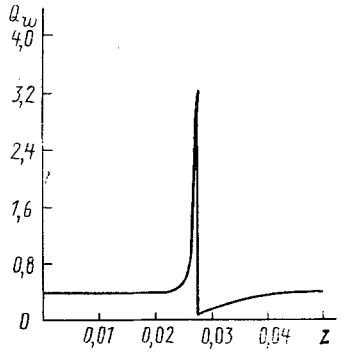


Fig. 2

Fig. 1. Vapor–drop flow parameter distribution along channel length under steady-state conditions (at z = 0: ρW = 380 kg/(m²·sec), Q = 92 kW, ΔT = 40°C): heat removal by vapor $Q_{W1}$ and drops $Q_{W2}$, J/(m²·sec); heated surface temperature $T_W$ and vapor temperature $T_1$, K; z, m.

Fig. 2. Characteristic profile of thermal flux into mixture in vicinity of heat liberation crisis, MW/m².

The cofactor d/(4δ) of $Q_W$ is explained by the fact that in Eq. (4) all terms are referred to a unit volume of the metal from which the tube is made (1Kh189T stainless steel), while the quantity $Q_W$ (introduced previously) is referenced to a unit of mixture volume. Heat liberation from the tube walls into the surrounding medium is not considered (for the conditions considered thermal losses into the surrounding medium, as shown by calculations using the engineering recommendations of [7], do not exceed 2-3%). The thermophysical data for stainless steel 1Kh189T were determined by approximating the tabular data of [8].

The thermal flux into the mixture $Q_W$ in the pre-crisis heat exchange region was calculated with the expression presented in [9], while in the post-crisis region (vapor–drop flow zone) the present model was used. For boundary conditions it was assumed that the temperature upon transition from the left of the crisis front was equal to the heated surface temperature in the pre-crisis heat exchange region, while for transition from the right of the crisis front the temperature was assumed equal to that in the post-crisis heat exchange region.

As initial conditions for Eq. (4) a distribution $T_W$ corresponding to steady conditions (obtained by solution of Eq. (4) without consideration of time derivatives) was used. It should be noted that under nonsteady conditions in many cases a heat liberation crisis and vapor–drop flow did not develop at the initial moment and Eq. (4) was not used. Equation (4) was approximated by the simplest possible implicit finite difference equation [10], which was then solved by the drive method. An iteration technique was used: in step i the thermal flux into the mixture was represented as a linear function of temperature, with the coefficients found from the temperature profile obtained in iteration i − 1. It should be noted that these coefficients change significantly with change in temperature. The accuracy of the calculations was verified by checking conservation of energy and performing calculations on finer grids. Calculations showed that when the calculation region was divided into 100 cells the error does not exceed several percent.

Figure 2 shows the profile of thermal flux into the mixture, obtained by numerical solution of Eq. (4) for a steady-state vapor–drop flow under the same conditions as shown in Fig. 1. It is evident from the figure that heat liberation increases abruptly in the pre-crisis region upon approach to the location of the crisis front and falls at the beginning of the post-crisis region to a value significantly less than the mean heat liberation. This is explained by heat transport from the post-crisis region into the pre-crisis one.

The proposed model was used to process various experiments on channel heating with flow of vapor–liquid mixtures. As an example we will present data on a subsequent experiment [7], modeling an accidental situation in energy generation equipment. At the initial moment in the heated tube (length L = 7 m, d = 10 mm, wall thickness δ = 1 mm) a mixture moved under

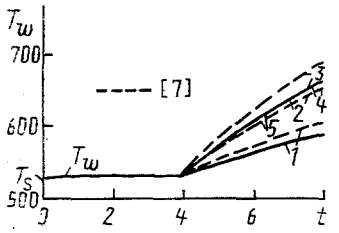


Fig. 3

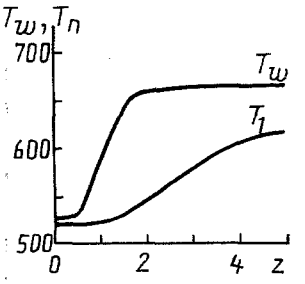


Fig. 4

Fig. 3. Time dependence of experimental (dashes) and calculated (solid lines) channel wall temperature values at points of thermocouple insertion, K. Curves 1-5 correspond to distances from channel input of 925, 2733, 1375, 3483, and 4233 mm. t, sec.

Fig. 4. Distribution of wall $T_w$ and vapor $T_1$ temperatures over channel length at time t = 8 sec. $T_n$, K.

following steady conditions: total thermal flux Q = 40 kW, pressure at channel input (at z = 0) p = 30 bar, specific mass flow rate (at z = 0) $\rho W$ = 2100 kg/(m²·sec), liquid underheat at channel input (at z = 0) $\Delta T$ = 20°C. The parameters of the underheated liquid at the tube input completely determine the motion of the vapor–liquid flow at t = 0. During the course of the experiment the mass flow rate $\rho W$ was decreased linearly from 2100 kg/(m²·sec) to 0, and then maintained equal to zero. The remaining parameters of the underheated liquid (p, $\Delta T$) at the tube input remained constant. For the situation considered these conditions form a complete boundary condition system. In this experiment active liquid evaporation in the channel was observed together with heating of the wall. Figure 3 shows a comparison of experimental [7] and calculated values of channel wall temperature. It is evident from the figure that at the moment of the heat liberation crisis the wall temperature change at the crisis point reaches hundreds of degrees per second. It is also evident that the calculated wall temperature differs only slightly from the experimental. Some of the curves coincide, which implies equality of temperatures at different distances from the entrance. The calculations showed that upon heating of the channel walls the thermal flux into the mixture is much less than heat liberation into the channel walls. Figure 4 shows changes in wall and vapor temperature. It is evident from the figure that the wall temperature increases monotonically while the total by which the vapor is heated at the tube exit reaches 100°.

The numerical study of flow of a vapor–drop mixture in heated channels under conditions characteristic of energy generation devices performed above permits the following conclusions:

1. In the flow of a vapor–drop mixture a significant contribution to heat removal from the heated surface into the flow is produced by drops which gather heat upon collision with the heated surface. For steady state flow of vapor–drop mixtures in the post-crisis region two cases are possible. The first is that in which at the beginning of the vapor–drop flow heat removal by drops is much greater than heat removal by vapor. The drop flow rate decreases over channel length, as does heat removal from the heated surface by drops. Therefore, heat removal by vapor increases (since the sum of heat removal by drops and vapor is constant over channel length and equal to the heat supplied into the tube walls.). In this case the temperature of the heated surface increases along the channel length. The second case is that in which at the beginning of the vapor–drop flow heat removal by vapor is much greater than the heat removal by drops. Flow velocity then increases along the tube length which leads to a certain increase in the heat liberation coefficient between the heated surface and the vapor. Therefore, the temperature of the heated surface decreases somewhat along channel length.

2. In a vapor–drop flow, drop motion relative to the vapor has a significant effect on heat exchange between drops and vapor (neglect of the relative motion leads to errors by a factor of four times), although the velocity difference does not exceed 5% of the total flow velocity (and can be neglected in the momentum equation). The effect of the relative motion on heat exchange decreases with increase in the total flow rate of the vapor–drop mixture.

## NOTATION

$C_f$, $C_{1f}$, friction coefficients between vapor and drops and between vapor-drop flow and channel wall; $c_1$, $c_w$, heat capacity of vapor and steel, $m^2/(sec^2 \cdot K)$; $d_d$, drop diameter, m; $F_w$, friction force between vapor–drop flow and wall, referred to unit volume of mixture, $kg/(m^2 \cdot sec^2)$; g, acceleration of gravity, $m/sec^2$; $J_{ij}$, intensity of mass transition from phase i into phase j, relative to unit volume of mixture (i, j, phase numbers (i, j = 1, 2)), $kg/(m^3 \cdot sec)$; $\ell$, heat of evaporation, J/kg; $N_w$, quantity of drops departing from flow core into wall region per unit time per unit channel volume, $m^{-3} \cdot sec^{-1}$; n, number of drops per unit volume of mixture, $m^{-3}$; p, mixture pressure, bar; $Q_w$, thermal flux from heated surface to mixture per unit volume of mixture, $J/(m^3 \cdot sec)$; $Q_{wi}$, thermal flux from wall to phase i per unit volume of mixture, $J/(m^3 \cdot sec)$; $Q_{i\sigma}$, thermal flux from phase i to interphase boundary per unit volume of mixture, $J/(m^3 \cdot sec)$; $q_w$, heat liberation in tube walls per unit volume of metal, $J/(m^3 \cdot sec)$; $T_s$, saturation temperature, K; $T_2$, drop temperature, K; t, time, sec; $t_d$, drop oscillation period, sec; $u_i$, internal energy of phase i, J/kg; $u_{is}$, internal energy of phase i at saturation temperature, J/kg; v, vapor–drop flow velocity, m/sec; $v_{12}$, drop slippage relative to vapor, m/sec; z, coordinate along channel axis, m; $\alpha$, volume concentration; $\delta$, wall thickness, m; $\delta_*$, vapor interlayer thickness, m; $\lambda_1$, $\lambda_w$, thermal conductivities of vapor and steel, $J/(m \cdot sec \cdot K)$; $\mu_1$, $\mu_2$, vapor and liquid viscosities, $kg/(m \cdot sec)$; $\rho$, $\rho_w$, mixture and steel densities, $kg/m^3$; $\rho_i^0$, true density of phase i, equal to mass of phase i per unit volume of phase i, $kg/m^3$; $\sigma$, surface tension, $kg/sec^2$.

## LITERATURE CITED


1. R. I. Nigmatulin, Dynamics of Multiphase Media [in Russian], Vol. 2, Moscow (1987).
2. M. Kh. Ibragimov, V. I. Subbotin, V. P. Bobkov, et al., Turbulent Flow Structure and the Heat Transport Mechanism in Channels [in Russian], Moscow (1978).
3. M. Cumo, "Elementi di termotechnika del reattore," CNEN, Roma (1969).
4. A. W. Bennett, G. F. Hewitt, H. A. Kearsey, et al., "Heat transfer to steam water mixtures flowing in uniformly heated tubes in which the critical heat flux has been exceeded," AERE-R5373, Harwell, Great Britain, 21 (1967).
5. S. L. Rivkin and A. A. Aleksandrov, Thermophysical Properties of Water and Water Vapor [in Russian], Moscow (1980).
6. V. E. Kroshilin and Ya. D. Khodzhaev, Teplofiz. Vys. Temp., 25, No. 2, 323-328 (1987).
7. I. S. Dubrovskii, I. V. Elkin, A. Ya. Kramerov, et al., Safety Questions in Energy Transport and the Problems of Scientific Studies [in Russian], Moscow (1979), pp. 70-76.
8. N. B. Vargaftik, Thermophysical Properties of Materials [in Russian], Moscow (1956).
9. J. Delaye, M. Gio, and M. Ritmüller, Heat Exchange and Hydrodynamics in Atomic and Thermal Energy Production [Russian translation], Moscow (1984).
10. S. K. Godunov and V. S. Ryaben'kii, Difference Methods [in Russian], Moscow (1977).